RSC Advances

PAPER

View Article Online
View Journal | View Issue



Cite this: *RSC Adv.*, 2016, **6**, 62270

# Optimisation of conductive polymer biomaterials for cardiac progenitor cells†

C. Puckert,‡[a] A. Gelmi,‡[a] M. K. Ljunggren,[b] M. Rafat[c] and E. W. H. Jager*[a]

Received 5th May 2016
Accepted 21st June 2016

DOI: 10.1039/c6ra11682e

www.rsc.org/advances

The characterisation of biomaterials for cardiac tissue engineering applications is vital for the development of effective treatments for the repair of cardiac function. New 'smart' materials developed from conductive polymers can provide dynamic benefits in supporting and stimulating stem cells *via* controlled surface properties, electrical and electromechanical stimulation. In this study we investigate the control of surface properties of conductive polymers through a systematic approach to variable synthesis parameters, and how the resulting surface properties influence the viability of cardiac progenitor cells. A thorough analysis investigating the effect of electropolymerisation parameters, such as current density and growth, and reagent variation on physical properties provides a fundamental understanding of how to optimise conductive polymer biomaterials for cardiac progenitor cells.



## Introduction

The ability to direct adult stem cells into a specific lineage of cells is of high interest for tissue engineering, for instance for repairing cardiac function after the event of a myocardial infarction (MI). Fibrotic scar tissue produced after an MI causes impairment in the ability of the heart to pump blood, which is called ventricular remodelling.[1] As cardiac muscle cells are not regenerative in adults, introducing new cells onto the damaged tissue may improve cardiac function and prevent heart failure.[2–4] Cardiac stem cell therapy can in theory replace the contractile units that were lost after MI and it should be able to counter ventricular remodelling because the stem cells can 'reinforce' the scar, thereby changing its mechanical properties and thus preventing further ventricular dilatation. However, thus far clinical trials of cardiac stem cell therapy have been disappointing. They have shown no improvement of left ventricular function compared to control groups.[5] High stem cell mortality within the first few days after injection and low retention are major contributors to this lack of clinical efficacy.[4] In order to attain a successful implantation other delivery strategies are needed. One such strategy is to employ bio-engineered grafts or cardiac patches that will present the proper microenvironment to the stem cells to attach and survive. The microenvironment of the graft or patch is also a vital factor in tuning the stem cell differentiation; hence control of this microenvironment is the key to a successful cardiac patch.

Conductive polymers, namely polyanilines, polythiophenes, and polypyrroles, are experiencing a rapid increase in use for biomaterials in tissue engineering applications.[6–12] Several crucial properties of these polymers allow for fine-tuned control of the interaction between biomaterial and cell. Conductive polymers have excellent properties for use biomaterial applications, such as relative softness compared to conventional conductive materials (*i.e.* metals), high flexibility in preparation, and stability.[13–17] A secondary, but significant, aspect of these materials is their electrical conductivity.

Electrically conductive substrates provide passive benefits to cells which utilise electrical signalling; conductive carbon nanotube substrates have been demonstrated to facilitate the propagation of neural cell action potentials and signalling.[18,19] A conductive polymer (polyaniline) hydrogel scaffold also showed a passive improvement in nerve cell activity, *i.e.* adhesion, survival, and differentiation, due to the intrinsic electrical sensitivity.[20] Similarly to nerve and neural cells, cardiac cells are electroactive and hence the conductive nature of these conductive polymer can be influential as a passive substrate.

The conductive properties are also ideal for stimulating cells which react to electrical signals, such as muscle and nerve cells.[21–24] The electrochemical properties of the polymers also allows for mechanical actuation *via* the movement of ions during reduction and oxidation.[25] This combination of electrical and mechanical actuation creates a biomaterial that is capable of not only supporting cells, but also directly stimulating them. The direct stimulation of living cells is particularly interesting for the area of tissue engineering; research has shown that stem cells such as mesenchymal stem cells (MSCs)

[a]*Biosensors and Bioelectronics Centre, Dept of Physics, Chemistry and Biology (IFM), Linköping University, Linköping 581 83, Sweden. E-mail: edwin.jager@liu.se*

[b]*Integrative Regenerative Medicine Centre, Department of Clinical and Experimental Medicine, Linköping University, Linköping 581 85, Sweden*

[c]*Department of Biomedical Engineering, Linköping University, Linköping 581 85, Sweden*

† Electronic supplementary information (ESI) available. See DOI: 10.1039/c6ra11682e

‡ Equal contribution.

can differentiate from external stimulus such as electrical and mechanical. Mechanical stimulation has been applied to stem cells previously through cyclical mechanical strain, shear stress, and tensile stress.[26–31] This type of external stimulus is speculated to trigger or enhance the differentiation of stem cells through a combination of mechanical signalling *via* cell membrane receptors and through changes in cell transport.[32,33] The influence of electrical stimulation on the differentiation of cells has been proposed to occur *via* several mechanisms. The increased cell proliferation may be due to induced membrane depolarisation from the electrical stimulation, stimulating $Ca^{2+}$ ionic transport and upregulating gene pathways.[34] Polypyrrole (PPy) has been shown to be compatible with cardiac cells,[35,36] and has been used to directly stimulate cells *via* electrical[37,38] and mechanical[39,40] stimulus.

The electrochemical synthesis of PPy requires the presence of a dopant molecule, which is incorporated into the polymer structure during polymerisation.[41–43] All dopants will directly influence the physical properties of the resulting polymer material,[42,44,45] and in turn the physical properties of a surface will influence cellular behaviour. Stem cells have been observed to respond to changes in surface properties; topographical cues and cell-surface adhesion can influence the differentiation of stem cells.[46] The topographical state of the surface, ordered or disordered, can have a strong influence on the adhesion and cell activity of MSCs,[47] and also direct the fate of MSCs.[48] The physical properties of the substrate will influence the cell-surface interface *via* adhesion formations which in turn affect the cytoskeleton of the cell. The differentiation of stem cells involves restructuring of the cytoskeleton[49,50] and in turn manipulating the cytoskeleton through cell-surface interactions cell fate can be directed.[48]

A previous study that investigated the influence of different dopants on the biocompatibility of CPCs found that the change in the physical properties of the polymer material had a greater impact than the chemical properties of the dopants (*i.e.* biological activity of biomolecular dopants).[51] Here we study in greater detail the effects of synthesis parameters, such as current density, time, and reactant concentrations, have on the polymer properties. In turn we can more carefully control each property as a variable and subsequent influence on CPC biocompatibility.

We have chosen three different dopants which performed well in the previous study; chondroitin sulfate (CS), dodecylbenzenesulfonate (DBS), and *p*-toluene sulfonate (*p*TS). Each dopant has a different advantage. The biological active molecule CS was chosen due to its important role in coordinating attachment and adhesion to the extracellular matrix (ECM). CS has also been successfully used as a dopant for PPy in prior cellular research.[11,52–54] DBS has previously been shown to provide excellent actuative properties for PPy materials[55] and has good stability and high electrical conductivity, as well as success as a dopant for PPy *in vitro*.[16] The molecule *p*TS is a simple aromatic dopant commonly used to synthesize PPy with good material properties, such as high electrical conductivity and stability.[56] In addition, they have been extensively characterized with a broad variation of different cell types over the last years, providing good controls for comparison.

Initially the properties of PPy will be varied by changing several variable growth parameters such as growth time and current charge density, dopant concentration and monomer concentration. This study will examine how the changes of the physical properties of PPy will affect the cell response of CPCs, to determine which PPy material will be the optimal electroactive biomaterial for cardiac patch applications.

# Results

## Parameters

**Dopants.** When synthesised with the same growth parameters each dopant produced polymers with different roughness values (selected values in Fig. 1A). PPy(DBS) had a higher roughness compared to the two other dopants, ranging from 31 ± 11 nm to 473 ± 35 nm (data provided in ESI†). In comparison the roughness values for PPy(CS) ranged from 7 ± 1 nm to 249 ± 58 nm. Both PPy(DBS) and PPy(CS) displayed a greater change in surface roughness with changing growth parameters, in contrast to PPy(*p*TS) which had a much smaller range of roughness values (8 ± 1 nm to 60 ± 14 nm). When prepared with the same growth parameters, the contact angle measurements of each PPy(dopant) decreased in order of: DBS > *p*TS > CS as seen in Fig. 1B, a trend consistent with previous studies.[11] The materials prepared with dopant DBS had the highest contact angle values, which is indicative of a low surface energy. The contact angle values (data provided in ESI†) for PPy(DBS) ranged from 62 ± 1° to 102 ± 7°. PPy(*p*TS) had lower contact angle values than PPy(DBS), with values ranging from 36 ± 1° to 51 ± 6°. PPy(CS) was measured to have the lowest contact angle values with values ranging from 14 ± 1° to 41 ± 1°. Previous studies have shown that PPy(CS), as a highly charged polyanion, results in more hydrophilic polymers compared to *p*TS and DBS doped PPy.[11] The long, hydrophobic alkyl chain tail of the DBS anion is a assumed to be responsible for the higher contact angle measurements for the PPy(DBS) polymer.

The surface morphology of each selected polymer was also imaged using SEM to observe structural differences. The morphologies of PPy(*p*TS), PPy(CS) and PPy(DBS) were quite similar, each with typical nodular surface structures (Fig. 3). The average diameter of the nodules was ~10 μm for PPy(CS) (Fig. 3B(i)), compared to ~3 μm PPy(DBS) (Fig. 3C(i)). In the case of PPy(CS) for 60 min at 0.5 mA $cm^{-2}$ (Fig. 3A(i)), the image showed an irregular nodular structure.

**Electrodeposition charge.** Current density (mA $cm^{-2}$) and growth time (sec) are directly proportional to electrodeposition charge (mC $cm^{-2}$) during polymerisation. As the electrodeposition charge ($Q_D$) increases, the amount of PPy deposited will increase; a longer growth time allows the polymerisation reaction to continue to produce the polymer, and a higher current density increases the rate of the polymerisation reaction. As expected, increasing the $Q_D$ results in the thickness of the polymer increasing in a linear relationship for all dopants (see ESI†). As the thickness of the polymer increases, *i.e.* more

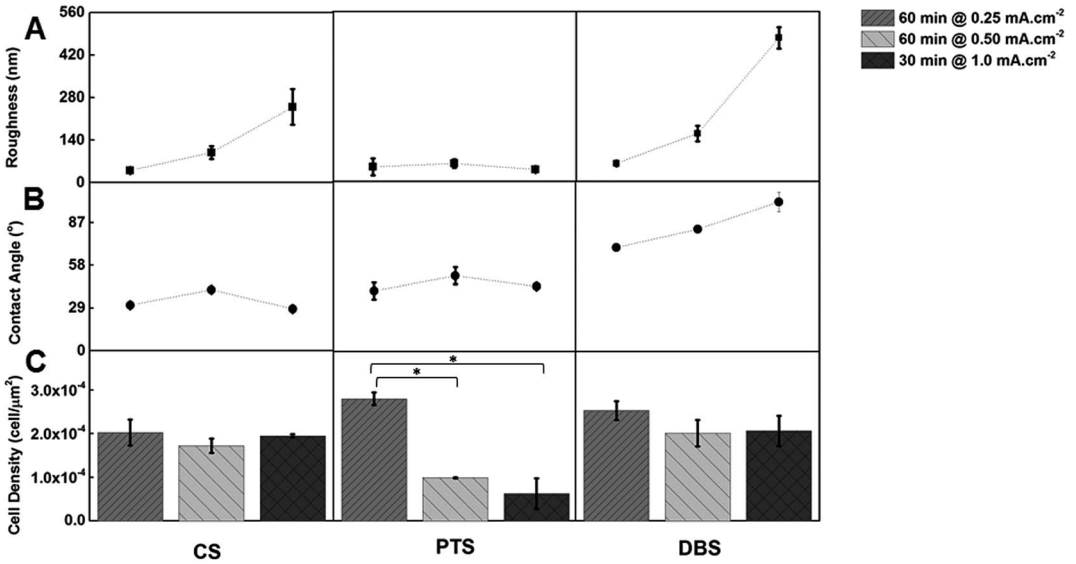


Fig. 1 Comparing the physical surface properties with CPC density where; (A) roughness (B) contact angle, and (C) cell density values for the dopants CS, *p*TS, and DBS at each growth parameter set of 60 min at 0.25 mA $cm^{-2}$, 60 min at 0.5 mA $cm^{-2}$, and 30 min at 1 mA $cm^{-2}$. *$p < 0.01$.

polymer deposited, it has been observed that the size of the nodular surface features also increases.[45] The increase in size of these nodules will contribute to the increasing roughness of the polymer surface and in general an increase in $Q_D$ correlates to an increase in roughness.[57] This effect observed here as all dopants increase in roughness with $Q_D$; for example, PPy(CS) grown at 0.25 mA $cm^{-2}$ for 60 minutes ($Q_D = 900$ mC $cm^{-2}$) had a roughness of 40 ± 6 nm, compared to 1 mA $cm^{-2}$ for 30 minutes ($Q_D = 1800$ mC $cm^{-2}$) with a roughness of 250 ± 58 nm (Fig. 1A).

The contact angle values did not have a strong correlation with an increase in $Q_D$, however for PPy(DBS) there was a general increase in contact angle with $Q_D$ (Fig. 1B). The contact angle increased from 71 ± 2° ($Q_D = 900$ mC $cm^{-2}$) to

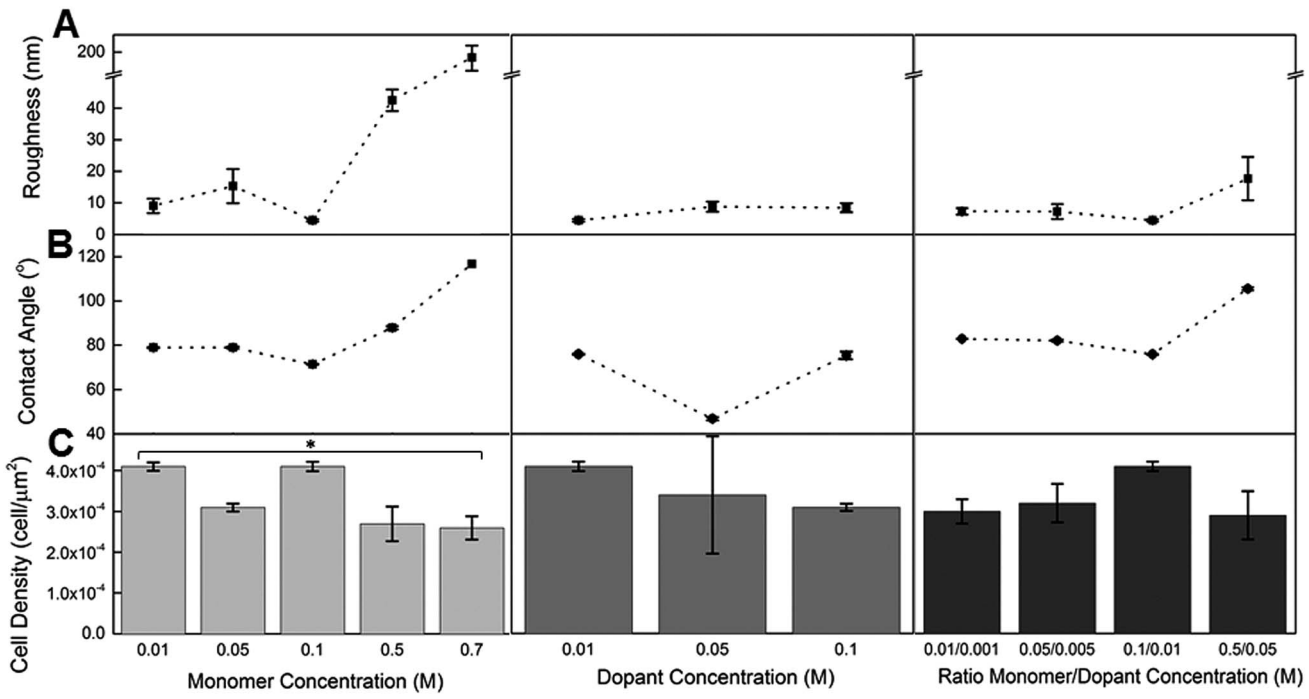


Fig. 2 Comparing the physical surface properties with CPC density where; (A) roughness (B) contact angle, and (C) cell density values for the variable monomer and constant dopant concentration, constant monomer and variable dopant concentration, and an increasing ratio of monomer and dopant concentration. *$p < 0.01$.

 

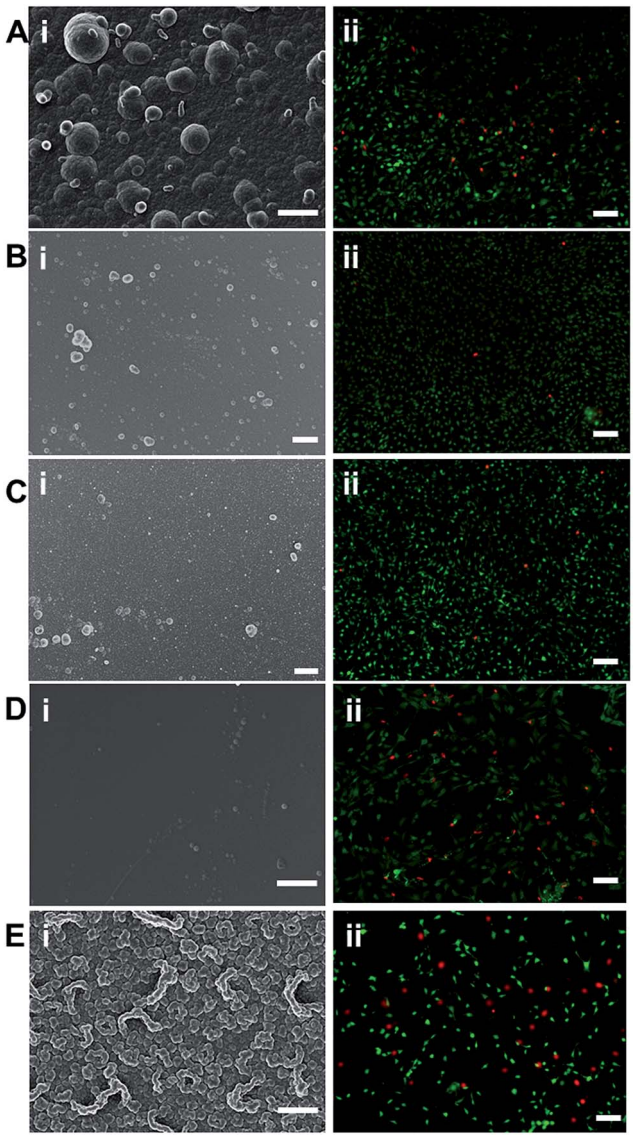


Fig. 3 (A) PPy(CS) 0.5 mA $cm^{-2}$ at 60 min, (B) PPy(*p*TS) 0.5 mA $cm^{-2}$ at 60 min, (C) PPy(DBS) 0.5 mA $cm^{-2}$ at 60 min, (D) 0.01 M Py DBS, 0.1 M Py, (E) 0.01 DBS, 0.7 Py. (i) SEM micrograph, scale bar 10 μm, (ii) Live/Dead staining CPC, scale bar 50 μm.

102 ± 7° ($Q_D$ = 1800 mC $cm^{-2}$). As the roughness values and contact angle measurements do not have a strong correlation, it can be assumed that the contact angle measurements are not impacted by surface morphology and more strongly influenced by the surface energy results from the polymer structure.

**Dopant and monomer concentration.** In order to discriminate the influence of the monomer and of the dopant, the concentrations were varied in a systematic manner and the resulting polymer characterised. The concentrations were varied as the following; constant monomer and varied dopant, varied monomer and constant dopant, and a fixed ratio between dopant and monomer concentration. Increasing the monomer concentration resulted in a sharp increase of roughness, as shown in Fig. 2A. The highest monomer concentration of 0.7 M Py had a roughness of 189 ± 25 nm, compared to the lowest concentration of 0.01 M Py with a roughness of 9 ± 2 nm. This roughness increase occurs due to the increased availability of the monomer for faster synthesis kinetics during electropolymerisation. The polymers with an increasing ratio of dopant : monomer show also that a high monomer concentration results in an increased roughness value (18 ± 7 nm), compared to lower monomer concentration (4.5 ± 0.4 nm, 7 ± 2 nm, 7 ± 1 nm) regardless of the dopant concentration. This is as expected as the amount of dopant incorporated into the polymer is dependent on the oxidation state of the PPy chains during electropolymerisation. For variable dopant concentration there is no substantial change in roughness, with roughness values ranging from 4.5 ± 0.4 nm to 9 ± 2 nm with an increasing concentration.

In correlation with the roughness values, the morphology of the polymer surface was observed to change markedly with increasing monomer concentration. Fig. 3D(i) shows a relatively smooth and flat surface topography for a polymer prepared with 0.01 M Py and 0.01 M DBS. The comparatively large increase in monomer concentration to 0.7 M Py (with the same concentration of DBS) produced a surface with 'wormy' structures that would contribute to the polymer's high roughness value (189 ± 25 nm). This morphology has been observed before when polymerising with high monomer concentrations.[58] The surface morphology of the rest of the polymers for this variable set displayed the typical 'cauliflower' surface structure and are similar in morphology (see ESI†).

The PPy(DBS) materials with an increasing scale of monomer and dopant concentration did not show a large variation in the contact angle measurements (range of 72° ± 1 to 78 ± 1°) until the monomer concentration was increased to 0.5 M, drastically increasing the contact angle measurement to 98 ± 1° (Fig. 2B). This result was also observed for an increasing monomer concentration with a set dopant concentration (0.01 M); the contact angle measurement for the lower concentrations of 0.01 M, 0.05 M, and 0.1 M were 79 ± 1°, 79 ± 1°, and 72 ± 1° respectively. Once the monomer concentration increased to 0.5 M and 0.7 M the contact angle values increased to 88 ± 1° and 117 ± 1° respectively. These measurements indicate that the high roughness values for these materials with high dopant concentration is a contributing factor to the increase in the contact angle. In comparison, a low dopant concentration of 0.05 M with a set monomer concentration of 0.1 M resulted in the lowest contact angle value measured for a PPy(DBS) film (46 ± 1°). Once the dopant concentration was increased the contact angle increased to 72 ± 0° for 0.1 M. It is interesting to notice that the roughness of the 0.05 M and 0.1 DBS films were comparable (9 ± 2 nm and 8 ± 1 respectively), while the contact angle differed more greatly. These observations suggest that the chemistry of the dopant is the controlling factor of surface energy for materials with a low roughness (<20 nm).

**Electroactivity.** The electroactive response of the polymer will be influenced by the dopant, and by growth and concentration variables. The three dopants have similar CV profiles (Fig. 4A), showing a capacitive response that is typical for PPy films. As electrodeposition charge is increased, the capacitance of the materials was also observed to increase which is expected

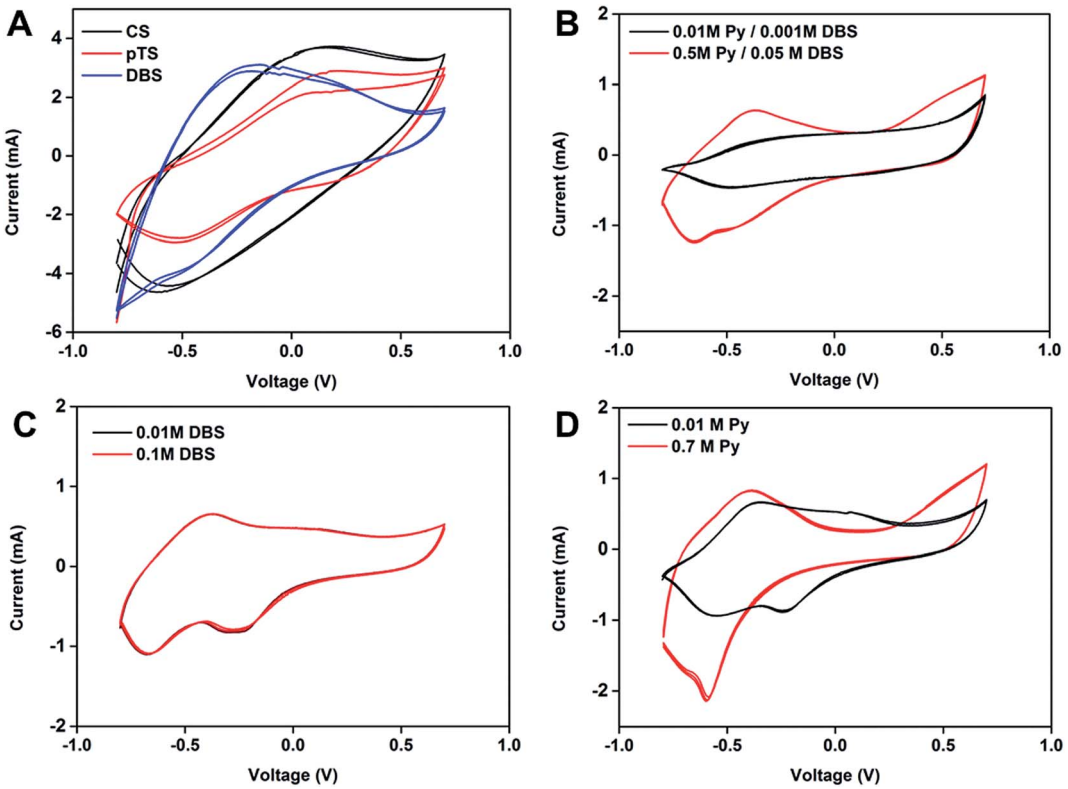


Fig. 4 Cyclic voltammetry scans of polymer films in PBS, scan range 0.8 V to −0.8 V at a scan rate of 50 mV $s^{-1}$; (A) PPy(CS) (black), PPy(*p*TS) (red), and PPy(DBS) (blue) grown at 0.5 mA for 60 min monomer solution variations were compared with (B) 0.01 M Py/0.001 M DBS (black) and 0.5 M Py/0.05 M DBS (red), (C) 0.1 M Py with 0.01 M DBS (black) and 0.1 M DBS (red), and (D) 0.01 M DBS with 0.01 M Py (black) and 0.7 M Py (red).

with the increasing amount of PPy deposited (data not shown). The PPy(DBS) films of different monomer and dopant concentrations were also electrochemically analysed, and the concentration of Py monomer was observed to have an effect on the electroactive response of the PPy(DBS) films. As the ratio of monomer : dopant was increased, the redox peaks of PPy became visibly apparent in the CV (Fig. 4B); however for the PPy(DBS) films prepared with 0.01 M and 0.1 M DBS, and a constant Py concentration of 0.1 M, the CVs were identical (Fig. 4C). Increasing the Py concentration from 0.01 M to 0.7 M, with 0.01 M DBS, showed an increase in the current at the redox peaks (Fig. 4D). The secondary redox peaks visible in the CV scans are due to the kinetic consequence of slow reduction processes which have been observed before in PPy materials for low anodic potentials.[60] The electroactivity of the polymers is important as the passive conducting ability of the PPy can assist in cardiac cell propagation and signalling, as discussed above.

**Cell viability and response.** In order to assess the influence of variables such as dopant, roughness, and surface energy on cellular growth we selected polymers from the parameter variation experiments for further cell biocompatibility experiments. Polymers with the similar physical properties but different dopant were chosen, as well as polymers with the same dopant but different physical properties in an aim to control the different variables. This included polymers grown 60 minutes at 0.25 mA $cm^{-2}$, 60 minutes at 0.5 mA $cm^{-2}$, and 30 minutes at 1 mA $cm^{-2}$. Their physical properties are displayed with cell density values in Fig. 1. All of the polymers with variable monomer solution concentrations were also assessed (Fig. 2).

The PPy(*p*TS) sample with the lowest current density (0.25 mA $cm^{-2}$, $Q_D = 900$ mC $cm^{-2}$) had the highest cell density value for the first set of samples with a value of $2.9 \pm 0.1 \times 10^{-4}$ $\mu m^{-2}$, and was significantly higher than the PPy(*p*TS) materials prepared at higher current densities (Fig. 1C). By way of comparison the control sample had a cell density of $3.4 \pm 0.4 \times 10^{-4}$ $\mu m^{-2}$ (cell culture plate). The polymers prepared with CS and DBS showed no significant difference in cell density within the variable current density set. The overall trend of increasing roughness with $Q_D$ has no significant influence on the cell density on the polymer materials, indicating that the magnitude of the roughness change induced by control of the synthesis parameters in this study/set is not high enough to adversely affect cellular adhesion and growth. Nanoscale roughness has been observed to have a significant influence on endothelial cells,[59] however this study demonstrates that the CPCs are less sensitive to the nanoscale changes in roughness observed for these materials. However drastic changes in the polymer structure and roughness for the high monomer concentration polymer (Fig. 3E) had a significant influence on the cell density. At 0.01 M Py the cell density value was $4.10 \pm 0.1 \times 10^{-3}$ $\mu m^{-2}$, significantly higher than the cell density for 0.7 M Py ($2.6 \pm 0.3 \times 10^{-4}$ $\mu m^{-2}$), which can be observed in Fig. 3D(ii) and E(ii).

 

This indicates that the CPCs are sensitive to $10^2$ roughness changes; however the cells are still viable on the surface demonstrating their ability to still adhere and propagate on the rougher surface.

Each polymer-dopant material fell within a discrete range of contact angle values, with all values indicating a hydrophilic surface. The CPC densities on these materials showed no indication of a preference for a particular range of contact angle, suggesting that the hydrophilic nature of the polymers was sufficient for cellular adhesion and growth. The high dopant concentration polymer, which had a contact angle of $117 \pm 1°$, is the only material with a more hydrophobic surface, and with a significantly lower cell density compared to the lower dopant concentration polymer as previously discussed above. Distinguishing the factors of roughness and contact angle in regards to the reduced cell density is difficult. It is not possible to determine whether the CPCs are sensitive to the increased roughness and irregular morphology of the material or the increased hydrophobicity of the surface with the data presented here. However for hydrophilic surfaces it can be determined that CPCs are not sensitive to changes in the degree of the surface energy.

## Conclusions

This study shows that the three dopants used during the PPy synthesis will produce variable but controllable changes of the physical properties of PPy materials. Further changes of the physical properties of the polymer can also be controlled through the growth parameters in order to create a set of materials with different properties such as roughness, surface energy, and morphology. Each dopant resulted in different physical properties for the resulting polymer, as expected, and it was observed that the hydrophobicity increased with the trend CS < *p*TS < DBS but was generally independent of electrodeposition charge. Conversely the roughness of the polymers was more influenced by the electrodeposition charge than individual dopants, with a higher electrodeposition charge resulting in rougher PPy polymers. Together with a CPC viability study the degree of influence and sensitivity the CPCs had to changes in the physical properties was analysed. In terms of the compatibility of the PPy films synthesized from various dopants, and in general DBS was found to produce PPy films with high biocompatibility and cell viability for CPCs. The CPCs did not demonstrate sensitivity to the nanoscale changes in roughness of the polymers, nor to changes with the hydrophilic range of contact angle measurements. However more large scale changes in roughness, morphology, and surface energy did reduce the cell density of the CPCs. This study indicates that the PPy materials produced are a suitable surface for the growth of CPCs, and that the CPCs are not sensitive to small scale changes in the material properties. This is promising for the further development of PPy as a material for cardiac patch applications, as the overall biocompatibility of the material will not be influenced through manipulation of the polymer to further optimise other properties, such as conductivity or flexibility.

## Experimental

### Polymer synthesis

The PPy polymer was synthesized using electrochemical polymerization in a 3 electrode electrochemical cell using a Ag/AgCl reference electrode (BASi, USA). The gold wafer working electrode was cleaned with ethanol and subsequently rinsed with Milli-Q water (18 MΩ).

The first set of polymers used three different dopants. For the polymerization processes the aqueous monomer solution contained 0.1 M Py and 2 mg $ml^{-1}$ of the appropriate dopant. The dopants used were chondroitin sulfate A sodium salt (Sigma-Aldrich), dodecylbenzenesulfonic sodium salt (TCI Europe), and sodium *para*-toluenesulfonate (Sigma-Aldrich). After the polymerization the sample was cleaned with Milli-Q water and dried with $N_2$. The properties of the PPy were changed by controlling the current density and the time of polymerization for each of the three dopants. The growth time range included 1, 10, 30, and 60 min. The current density range included 0.25, 0.5, 1, and 5 mA $cm^{-2}$.

The second set of polymers were produced using DBS as a dopant, and the properties were changed by controlling the concentration of the dopant and the monomer. The growth parameters used were 0.25 mA $cm^{-2}$ current density and 10 min growth time. The dopant concentrations used were 0.001, 0.005, 0.01, and 0.05 M. The monomer concentrations used were 0.01, 0.05, 0.1, 0.5, and 0.7 M. Three subsets of polymer were synthesised using dopant : monomer ratio (1 : 10), monomer concentration (0.1 M) with variable dopant concentration, and dopant concentration (0.01 M) with variable monomer concentration.

### Contact angle goniometry

A CAM200 Optical Contact Angle Meter (KSV Instruments, Finland) was used for the comparative evaluation of the surface energy of PPy. The sessile drop method using Milli-Q water (18 MΩ) was used to measure the interface angle. For each film, three samples were analyzed by measuring the left and right angle of the drop ten times.

### Profilometry

The roughness of the polymer films was measured using a Dektak 6 M profilometer (Veeco Instruments Inc., NY). The roughness was investigated by measuring the surface three times per sample over a length of 5000 μm with a stylus force of 3 mg.

### Scanning electron microscope

The surface morphologies of the selected PPy films were obtained by using a high-resolution Scanning Electron Microscope (SEM). The PPy samples were examined in the LEO 1550 scanning electron microscope (Zeiss, Germany) with an electron beam energy of 5.02 kV.

### Cyclic voltammetry

The electroactivity of the selected PPy films was measured using cyclic voltammetry with a potentiostat (Ivium, Netherlands). The PPy films were analysed using a 3 electrode electrochemical cell using a Ag/AgCl reference electrode (BASi, USA), stainless steel mesh counter-electrode, in 0.1 M NaDBS aqueous solution and cycled from 0.8 V to −0.8 V at a rate of 50 mV $s^{-1}$.

### Cell culture

CPCs were isolated from the hearts of adult mice using a cardiac stem cells isolation kit (Millipore). The maintenance medium used was Dulbecco's Modified Eagle Medium: nutrient mixture F-12 (DMEM/F12) (Sigma-Aldrich) supplemented with 10% FCS, 1% penicillin – streptomycin (Invitrogen), 1× insulin-transferrin-selenium (ITS) (Invitrogen), 0.5% DMSO (Sigma-Aldrich) and 20 ng $ml^{-1}$ epidermal growth factor (EGF) (Invitrogen).

All PPy samples were firstly incubated overnight in 5× concentrated penicillin-streptomycin solution followed by thorough washing with sterile PBS aqueous solution. The CPCs on the PPy films were then incubated for 24 h in sterile antibiotic-free medium to check the efficacy of the bacterial decontamination. If no microbial growth was observed, the PPy films were used for cell culture testing. All decontaminated biomaterials samples were place on the bottom of a 12-well cell culture plate and 1 ml of the cell maintenance medium was added. CPCs were collected by trypsinization and seeded at a density of $5 \times 10^4$ cells per well. Additionally, the same amount of CPCs was seeded in empty wells, these served as control samples.

After 3 days of culture, once the control sample became confluent, a Live/Dead Assay LIVE/DEAD® Viability/Cytotoxicity Kit (Life Technologies, cat. no. L-3224) was used to investigate cell adhesion, viability, and proliferation rate and assessed with an inverted fluorescent microscope AXIO CAM ICm1 (Zeiss, Germany). Cell numbers were quantified using the cell count function in ImageJ (NIH). At least 2 fields were counted per sample. Statistical analysis was performed using 1-way ANOVA and student *t*-test (two tail). Representation of significance is denoted: $*p < 0.01$.

## Acknowledgements

We would like to acknowledge Prof. May Griffith and Linköping Integrative Regenerative Medicine Centre (IGEN), Linköping University, for the supply of the progenitor cells and cell facilities. Prof. Anthony Turner is acknowledged for his support. Financial support was received from Linköping University, IGEN (post-doc grant), COST-Action MP1003, Knut och Alice Wallenberg Commemorative Fund, and the European Research Agency for EU FP7-PEOPLE-2011-CIG-Marie Curie Actions-Career Integration Grant (CIG).

## Notes and references

1 M. A. Konstam, D. G. Kramer, A. R. Patel, M. S. Maron and J. E. Udelson, *JACC: Cardiovascular Imaging*, 2011, **4**, 98–108.
2 J. Leor, S. Aboulafia-Etzion, A. Dar, L. Shapiro, I. M. Barbash, A. Battler, Y. Granot and S. Cohen, *Circulation*, 2000, **102**, III-56–III-61.
3 P. Zammaretti and M. Jaconi, *Curr. Opin. Biotechnol.*, 2004, **15**, 430–434.
4 J. V. Terrovitis, R. R. Smith and E. Marbán, *Circ. Res.*, 2010, **106**, 479–494.
5 C. L. Mummery, R. P. Davis and J. E. Krieger, *Sci. Transl. Med.*, 2010, **2**, 27ps17.
6 P. R. Bidez, S. Li, A. G. MacDiarmid, E. C. Venancio, Y. Wei and P. I. Lelkes, *J. Biomater. Sci., Polym. Ed.*, 2006, **17**, 199–212.
7 A. Borriello, V. Guarino, L. Schiavo, M. Alvarez-Perez and L. Ambrosio, *J. Mater. Sci.: Mater. Med.*, 2011, **22**, 1053–1062.
8 A.-D. Bendrea, L. Cianga and I. Cianga, *J. Biomater. Appl.*, 2011, **26**, 3–84.
9 R. D. Breukers, K. J. Gilmore, M. Kita, K. K. Wagner, M. J. Higgins, S. E. Moulton, G. M. Clark, D. L. Officer, R. M. I. Kapsa and G. G. Wallace, *J. Biomed. Mater. Res., Part A*, 2010, **95A**, 256–268.
10 D. D. Ateh, H. A. Navsaria and P. Vadgama, *J. R. Soc., Interface*, 2006, **3**, 741–752.
11 K. J. Gilmore, M. Kita, Y. Han, A. Gelmi, M. J. Higgins, S. E. Moulton, G. M. Clark, R. Kapsa and G. G. Wallace, *Biomaterials*, 2009, **30**, 5292–5304.
12 Z.-B. Huang, G.-F. Yin, X.-M. Liao and J.-W. Gu, *Front Mater Sci*, 2014, 1–7, DOI: 10.1007/s11706-014-0238-8.
13 N. Guimard, N. Gomez and C. Schmidt, *Prog. Polym. Sci.*, 2007, **32**, 876–921.
14 R. A. Green, N. H. Lovell, G. G. Wallace and L. A. Poole-Warren, *Biomaterials*, 2008, **29**, 3393–3399.
15 K. Svennersten, M. H. Bolin, E. W. H. Jager, M. Berggren and A. Richter-Dahlfors, *Biomaterials*, 2009, **30**, 6257–6264.
16 V. Lundin, A. Herland, M. Berggren, E. W. H. Jager and A. I. Teixeira, *PLoS One*, 2011, **6**, e18624.
17 J. Y. Wong, R. Langert and D. E. Ingberi, *Science*, 1994, **91**, 3201–3204.
18 V. Lovat, D. Pantarotto, L. Lagostena, B. Cacciari, M. Grandolfo, M. Righi, G. Spalluto, M. Prato and L. Ballerini, *Nano Lett.*, 2005, **5**, 1107–1110.
19 S. Agarwal, X. Zhou, F. Ye, Q. He, G. C. K. Chen, J. Soo, F. Boey, H. Zhang and P. Chen, *Langmuir*, 2010, **26**, 2244–2247.
20 V. Guarino, M. A. Alvarez-Perez, A. Borriello, T. Napolitano and L. Ambrosio, *Adv. Healthcare Mater.*, 2013, **2**, 218–227.
21 M. Bolin, K. Svennersten, D. Nilsson, A. Sawatdee, A. Richter-Dahlfors, E. W. H. Jager and M. Berggren, *Adv. Mater.*, 2009, **21**, 4379–4382.
22 S. Dusterhoft and D. Pette, *Differentiation*, 1990, **44**, 178–184.
23 A. F. Quigley, J. M. Razal, M. Kita, R. Jalili, A. Gelmi, A. Penington, R. Ovalle-Robles, R. H. Baughman, G. M. Clark, G. G. Wallace and R. M. I. Kapsa, *Adv. Healthcare Mater.*, 2012, **1**, 801–808.
24 C. E. Schmidt, V. R. Shastri, J. P. Vacanti and R. Langer, *Proc. Natl. Acad. Sci. U. S. A.*, 1997, **94**, 8948–8953.
25 M. R. Gandhi, P. Murray, G. M. Spinks and G. G. Wallace, *Synth. Met.*, 1995, **73**, 247–256.

 

26 N. Shimizu, K. Yamamoto, S. Obi, S. Kumagaya, T. Masumura, Y. Shimano, K. Naruse, J. K. Yamashita, T. Igarashi and J. Ando, *J. Appl. Physiol.*, 2008, **104**, 766–772.
27 C. A. Simmons, S. Matlis, A. J. Thornton, S. Chen, C.-Y. Wang and D. J. Mooney, *J. Biomech.*, 2003, **36**, 1087–1096.
28 J. S. Park, J. S. Chu, C. Cheng, F. Chen, D. Chen and S. Li, *Biotechnol. Bioeng.*, 2004, **88**, 359–368.
29 D. F. Ward Jr, R. M. Salasznyk, R. F. Klees, J. Backiel, P. Agius, K. Bennett, A. Boskey and G. E. Plopper, *Stem Cells Dev.*, 2007, **16**, 467–480.
30 N. Datta, Q. P. Pham, U. Sharma, V. I. Sikavitsas, J. A. Jansen and A. G. Mikos, *Proc. Natl. Acad. Sci. U. S. A.*, 2006, **103**, 2488–2493.
31 M. R. Kreke, L. A. Sharp, Y. Woo Lee and A. S. Goldstein, *Tissue Eng., Part A*, 2008, **14**, 529–537.
32 I. Titushkin, S. Sun, J. Shin and M. Cho, *J. Biomed. Biotechnol.*, 2010, **2010**, 1–14.
33 K. Kurpinski, J. Park, R. G. Thakar and S. Li, 2006.
34 A. S. Rowlands and J. J. Cooper-White, *Biomaterials*, 2008, **29**, 4510–4520.
35 M. Nishizawa, H. Nozaki, H. Kaji, T. Kitazume, N. Kobayashi, T. Ishibashi and T. Abe, *Biomaterials*, 2007, **28**, 1480–1485.
36 L. Jin, T. Wang, Z.-Q. Feng, M. Zhu, M. K. Leach, Y. I. Naime and Q. Jianga, *J. Mater. Chem.*, 2012, **22**, 18321–18326.
37 B. C. Thompson, R. T. Richardson, S. E. Moulton, A. J. Evans, S. O'Leary, G. M. Clark and G. G. Wallace, *J. Controlled Release*, 2010, **141**, 161–167.
38 X. Liu, K. J. Gilmore, S. E. Moulton and G. G. Wallace, *J. Neural. Eng.*, 2009, **6**, 065002.
39 K. Svennersten, M. Berggren, A. Richter-Dahlfors and E. W. H. Jager, *Lab Chip*, 2011, **11**, 3287–3293.
40 A. Gelmi, A. Cieslar-Pobuda, E. de Muinck, M. Los, M. Rafat and E. W. H. Jager, *Adv. Healthcare Mater.*, 2016, **5**, 1471–1480.
41 L. F. Warren and D. P. Anderson, *J. Electrochem. Soc.*, 1987, **134**, 101–105.
42 G. R. Mitchell, F. J. Davis and C. H. Legge, *Synth. Met.*, 1988, **26**, 247–257.
43 T. F. Otero and E. De-Larreta, *Synth. Met.*, 1988, **26**, 79–88.
44 A. Gelmi, M. J. Higgins and G. G. Wallace, *Biomaterials*, 2010, **31**, 1974–1983.
45 T. Silk, Q. Hong, J. Tamm and R. G. Compton, *Synth. Met.*, 2000, **93**, 59–64.
46 E. Ghafar-Zadeh, J. R. Waldeisen and L. P. Lee, *Lab Chip*, 2011, **11**, 3031–3048.
47 S. Bauer, J. Park, J. Faltenbacher, S. Berger, K. von der Mark and P. Schmuki, *Integr. Biol.*, 2009, **1**, 525–532.
48 M. J. Dalby, N. Gadegaard, R. Tare, A. Andar, M. O. Riehle, P. Herzyk, C. D. Wilkinson and R. O. Oreffo, *Nat. Mater.*, 2007, **6**, 997–1003.
49 J. D. Pajerowski, K. N. Dahl, F. L. Zhong, P. J. Sammak and D. E. Discher, *Proc. Natl. Acad. Sci. U. S. A.*, 2007, **104**, 15619–15624.
50 Y. Yoon, K. Pitts and M. McNiven, *Mol. Biotechnol.*, 2002, **21**, 241–250.
51 A. Gelmi, M. K. Ljunggren, M. Rafat and E. W. Jager, *J. Mater. Chem. B*, 2014, **2**, 3860–3867.
52 J. Serra Moreno, S. Panero, S. Materazzi, A. Martinelli, M. G. Sabbieti, D. Agas and G. Materazzi, *J. Biomed. Mater. Res., Part A*, 2009, **88**, 832–840.
53 J. Pelto, M. Bjorninen, A. Palli, E. Talvitie, J. Hyttinen, B. Mannerstrom, R. Suuronen Seppanen, M. Kellomaki, S. Miettinen and S. Haimi, *Tissue Eng., Part A*, 2013, **19**, 882–892.
54 J. S. Moreno, S. Panero, M. Artico and P. Filippini, *Bioelectrochemistry*, 2008, **72**, 3–9.
55 E. Smela and N. Gadegaard, *Adv. Mater.*, 1999, **11**, 953–957.
56 P. Murray, G. M. Spinks, G. G. Wallace and R. P. Burford, *Synth. Met.*, 1997, **84**, 847–848.
57 M. J. Higgins, S. T. McGovern and G. G. Wallace, *Langmuir*, 2009, **25**, 3627–3633.
58 A. Kaynak, *Mater. Res. Bull.*, 1997, **32**, 271–285.
59 T. F. Otero and M. J. Ariza, *J. Phys. Chem. B*, 2003, **107**, 13954–13961.
60 T.-w. Chung, D.-z. Liu, S.-y. Wang and S.-s. Wang, *Biomaterials*, 2003, **24**, 4655–4661.